

Review

Period-One Laser Dynamics for Photonic Microwave Signal Generation and Applications

Pei Zhou ^{1,2,3}, Nianqiang Li ^{1,2,*} and Shilong Pan ³ 

¹ School of Optoelectronic Science and Engineering, Soochow University, Suzhou 215006, China; peizhou@suda.edu.cn

² Key Lab of Advanced Optical Manufacturing Technologies of Jiangsu Province & Key Lab of Modern Optical Technologies of Education Ministry of China, Soochow University, Suzhou 215006, China

³ Key Laboratory of Radar Imaging and Microwave Photonics, Ministry of Education, Nanjing University of Aeronautics and Astronautics, Nanjing 210016, China; pans@nuaa.edu.cn

* Correspondence: nli@suda.edu.cn

Abstract: Due to the advantages of rich dynamics, small size, and easy integration, semiconductor lasers have many applications in microwave photonics. With a proper perturbation to invoke period-one (P1) nonlinear laser dynamics, a widely tunable microwave signal can be generated. In this paper, we concentrate on the realization and application of photonic microwave signal generation based on the P1 oscillation state of semiconductor lasers. Recent developments in P1 dynamics-based tunable microwave signal generation techniques are reviewed with an emphasis on the optical injection system, which has a large frequency tuning range that is far beyond the intrinsic relaxation oscillation frequency. In order to improve the spectral purity and stability of the generated microwave signal, two typical approaches are introduced, i.e., microwave modulation stabilization, and delayed feedback stabilization. Various applications of the P1 dynamics-based microwave signal generator in diverse signal generation and photonic microwave signal processing are described. Development trends of the P1 dynamics-based photonic microwave signal generator are also discussed.

Keywords: microwave photonics; semiconductor lasers; optical injection; period-one oscillation; nonlinear dynamics; microwave generation



Citation: Zhou, P.; Li, N.; Pan, S. Period-One Laser Dynamics for Photonic Microwave Signal Generation and Applications. *Photonics* **2022**, *9*, 227. <https://doi.org/10.3390/photonics9040227>

Received: 28 February 2022

Accepted: 22 March 2022

Published: 31 March 2022

Publisher's Note: MDPI stays neutral with regard to jurisdictional claims in published maps and institutional affiliations.



Copyright: © 2022 by the authors. Licensee MDPI, Basel, Switzerland. This article is an open access article distributed under the terms and conditions of the Creative Commons Attribution (CC BY) license (<https://creativecommons.org/licenses/by/4.0/>).

1. Introduction

A microwave signal source that produces a broadly tunable microwave signal with low phase noise and high stability is considered a key component in many microwave and millimeter-wave systems, ranging from wireless communication systems, modern instrumentation, and radars to electronic warfare systems [1–3]. In recent decades, in order to overcome the limitations of conventional electronic technologies in carrier frequency, bandwidth and electromagnetic interference, photonic generation of microwave signals has attracted extensive attentions [4–8]. Semiconductor lasers are compact, reliable, and efficient coherent light sources with high-speed modulation capabilities. In addition, semiconductor lasers are inherently nonlinear devices. With proper perturbations, rich dynamical states of semiconductor lasers can be invoked, including stable locking, periodic oscillation, regular pulsation, quasi-periodic pulsation, frequency-locking, chaotic oscillation, and chaotic pulsation [9–15]. The dynamical states of semiconductor lasers have been utilized for many photonic microwave applications, and these states can be well controlled by properly varying the perturbation parameters. For instance, the simplest state of stable locking has been applied in modulation bandwidth enhancement, chirp and noise reduction in semiconductor lasers [16]. Chaotic dynamics have been demonstrated for chaos secure communication, high-speed random number generation, chaotic radar and lidar [17–19]. When operating at the period-one (P1) oscillation state, an optical wave with a single-frequency microwave modulation is obtained, which is suitable for photonic microwave

signal generation [20]. In this paper, we focus on the realization and application of photonic microwave signal generation based on the P1 oscillation state of the optical injection system, whose microwave frequency is broadly tunable by varying the injection conditions, and the frequency tuning range is far beyond the intrinsic laser bandwidth.

In this review, we will first introduce P1 dynamics-based tunable microwave signal generation techniques based on an optically injected semiconductor laser (OISL). In Section 3, two typical approaches to improve the spectral purity and stability of the generated microwave signal are introduced, including microwave modulation stabilization, and delayed feedback stabilization. Various applications of the P1 dynamics-based microwave signal generator in diverse signal generation, and photonic microwave signal processing are described in Section 4. Finally, development trends of the P1 dynamics-based photonic microwave signal generator are also discussed.

2. Photonic Microwave Signal Generation Based on P1 Dynamics

Under proper perturbations, e.g., optical injection, optical feedback, and optoelectronic feedback, a semiconductor laser can operate at the P1 oscillation, which outputs an optical carrier with a single-frequency intensity modulation [21]. After photodetection, a broadly tunable microwave signal can be generated. Due to the advantages of wide frequency range, flexible control, and no need for electrical components, the optical injection scheme has become the most preferred scheme.

The schematic diagram of an optical injection system is shown in Figure 1. Two lasers are arranged in master-slave configuration for optical injection. A continuous-wave (CW) light with a frequency of f_m from the master laser (ML) is injected into the slave laser after passing through a variable optical attenuator (VOA), a polarization controller (PC) and an optical circulator (CIR). The slave laser (SL) is a single-mode semiconductor laser with a free-running frequency of f_s . Here, the polarization of ML and SL are matched through the PC to maximize the injection efficiency, and the optical injection strength is adjusted by the optical attenuator. The output signal of the injected slave laser is sent to a photodetector (PD) to implement optical-to-electrical conversion. The desired microwave signal can be obtained at the output port of the PD.

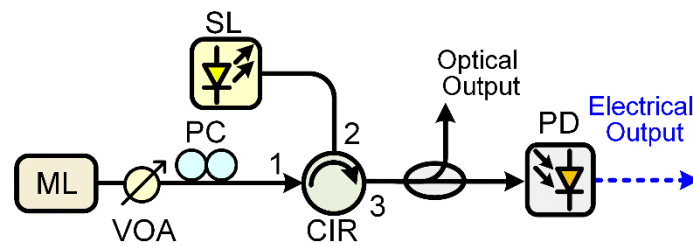


Figure 1. Schematic diagram of an optical injection system. ML: master laser; SL: slave laser; VOA: variable optical attenuator; PC: polarization controller; CIR: optical circulator; PD: photodetector.

The dynamics of the OISL system can be described by the rate equations between the intracavity optical field amplitude $A(t)$ and the charge carrier density $N(t)$ [22]:

$$\frac{dA}{dt} = \frac{1 - ib}{2}(g - \gamma_c)A + \gamma_c \xi_i |A_0| \exp(-i2\pi f_i t) + \chi \tag{1}$$

$$\frac{dN}{dt} = -\gamma_s(N - N_0) - \gamma_s J N_0 \left(\frac{g|A|^2}{\gamma_c |A_0|^2} - 1 \right) \tag{2}$$

where A_0 and N_0 are the free-running values of $A(t)$ and $N(t)$, respectively. The optical gain g is given by

$$g = \gamma_c + \frac{\gamma_c \gamma_n (N - N_0)}{\gamma_s J N_0} - \gamma_p \left(\frac{|A|^2}{|A_0|^2} - 1 \right) \tag{3}$$

In Equations (1)–(3), b is the linewidth enhancement factor, γ_c is the cavity decay rate, γ_s is the spontaneous carrier relaxation, γ_n is the differential carrier relaxation rate, γ_p is the nonlinear carrier relaxation rate, and J is the normalized bias current above the threshold. The optical injection is specified by the injection parameters (f_i, ζ_i) . Here, f_i is the detuning frequency of the ML with respect to the free-running SL, and ζ_i is the normalized optical injection strength. χ denotes the complex Langevin fluctuating force, which is used to characterize the spontaneous emission noise of SL [23]. Through adjusting the optical injection parameters, different dynamical states of the OISL system can be invoked, including stable locking, period-one, period-two and chaotic states [24]. In particular, we focus on the microwave generation and application characteristics of the period-one state.

Figure 2 presents the spectral characteristics of an OISL in the period-one oscillation state. P1 dynamics can be invoked through undamping the relaxation resonance of the semiconductor laser. The physical mechanism behind the P1 oscillation can be explained by the dynamical competition between injection-imposed laser oscillation and injection-shifted cavity resonance of the injected laser. On the one hand, the injection light at f_m pulls the intracavity field oscillation of the SL toward f_m by locking the optical phase of the laser, leading to the frequency component f_m at the laser output. On the other hand, the necessary gain of the slave laser is modified by optical injection. The refractive index inside the cavity changes through the antiguidance effect, resulting in the redshift of the cavity resonance from f_s toward f_s' [20]. Therefore, such injection-shifted cavity resonance competes dynamically with the injection-imposed laser oscillation, which radically modifies the dynamics of the injected laser. Under proper injection conditions, this would lead to the emergence of an asymmetric double-sideband (DSB) spectrum that is equally separated by the P1 oscillation frequency f_o ($f_o = f_m - f_s'$) through Hopf bifurcation. As illustrated in Figure 2, such a spectrum is a typical signature of P1 dynamics in OISLs [20–24]. After beating the optical components at a photodetector, a microwave signal with a fundamental frequency of f_o can be generated. Since the cavity resonance shift depends on the gain reduction, which is determined by the injection condition, the beating microwave frequency is dependent on the injection strength and the detuning frequency between the master and slave lasers. In Figure 3, the dependence of the P1 oscillation frequency f_o on the master-slave detuning frequency and the optical injection strength (f_i, ζ_i) is more clearly presented as a mapping [23]. In the region of the period-one oscillation state, by simply adjusting the detuning frequency and the injection strength, the fundamental microwave frequency f_o is broadly tunable from a few to over 60 GHz. Even higher frequencies, e.g., on the order of 100 GHz, can be generated by properly increasing ζ_i and/or f_i , enabling the possibility of reaching even the terahertz band [25].

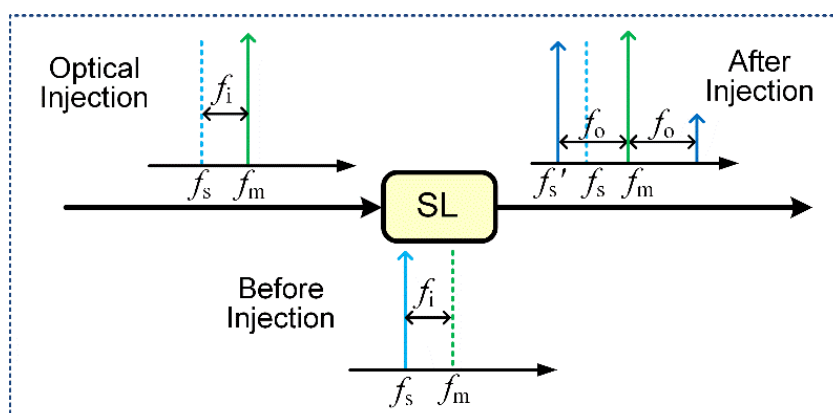


Figure 2. Illustration of typical spectral characteristics of an OSIL in the period-one state.

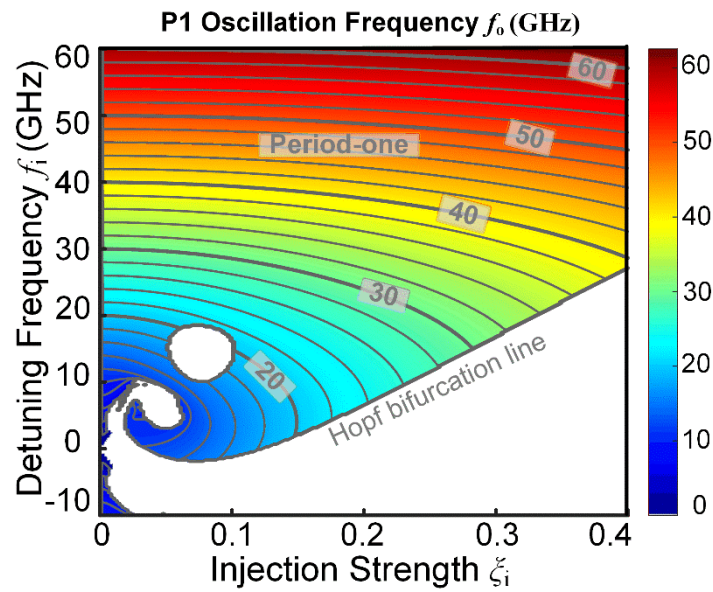


Figure 3. Dependence of the P1 oscillation frequency f_o on detuning frequency and injection strength [23].

Figure 4 presents the experimental results of tunable microwave signal generation based on the P1 oscillation of an OISL [26]. Figure 4a shows a typical optical spectrum of P1 dynamics (blue curve) when (f_i, ζ_i) equals (5.7 GHz, 0.84). For comparison, the spectra of the injection light (green curve) and the free-running SL (red curve) are also displayed. As can be seen, two highly dominant wavelength components separated by a P1 oscillation frequency of 21.5 GHz is observed after optical injection. Figure 4b plots the P1 frequency f_o as a function of the injection strength ζ_i when the detuning frequency f_i equals 5.7, 16.2, 25.7 and 35.5 GHz. As can be observed, for a fixed detuning frequency f_i , the P1 frequency f_o increases almost linearly with increasing injection strength ζ_i . In addition, the P1 frequency increases with increasing detuning frequency f_i for a fixed injection strength ζ_i . Here, a P1 frequency of approximately 9.6–46.6 GHz is measured, which is mainly limited by the bandwidth of the electrical spectrum analyzer. The corresponding electrical spectra of the generated microwave signals when $f_i = 5.7$ GHz are given in Figure 4c, and the frequency range is 9.6–22.6 GHz. These results prove the feasibility of using the P1 oscillation of an OISL as a photonic microwave source.

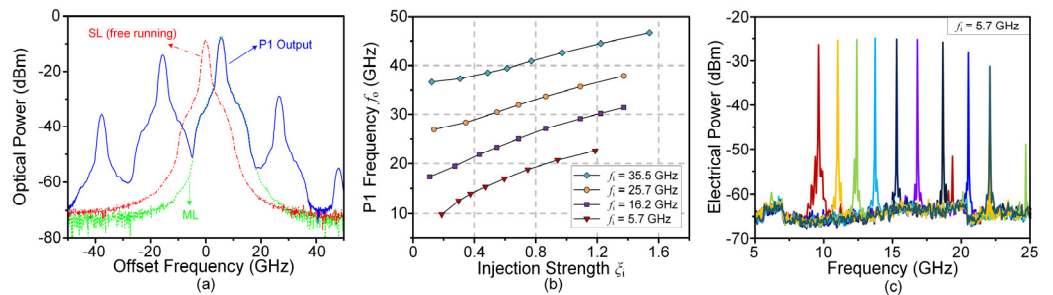


Figure 4. (a) Optical spectra of the injection light (green), the free-running SL (red), and the injected SL (blue) when (f_i, ζ_i) equals (5.7 GHz, 0.84); (b) P1 frequency f_o as a function of the injection strength ζ_i for different detuning frequencies f_i ; (c) electrical spectra when $f_i = 5.7$ GHz.

Apart from the aforementioned P1 dynamics-based method, a variety of photonic microwave signal generation schemes have been reported, including those based on external modulation [5], dual-frequency lasers [6], mode-locked lasers (MLLs) [7], and optoelectronic oscillators [8]. Table 1 presents a comparison of photonic microwave signal generation tech-

niques. As can be seen, compared with existing schemes, photonic microwave generation using the P1 oscillation of an OISL offers the following advantages.

Table 1. Comparison of Photonic Microwave Signal Generation Techniques.

| Techniques | Complexity | Cost | Tunability | Microwave Linewidth | Frequency Modulation |
|---------------------------|-------------|----------|------------|----------------------|-------------------------|
| External modulation | Moderate | High | Fair | Determined by source | Determined by source |
| Dual-frequency lasers | Moderate | Moderate | Fair | Moderate | No |
| Mode-locked lasers | Complicated | High | Poor | Narrow | No |
| Optoelectronic oscillator | Complicated | Moderate | Fair | Narrow | Special design required |
| Period-one dynamics | Simple | Low | Good | Moderate | Yes |

- (1) Simple Structure and Low Cost: The P1 oscillation generates photonic microwave signals all optically without using any microwave sources or high-speed modulators;
- (2) Good Frequency Tunability: The obtained microwave frequency f_o has a large frequency tuning range that is many times the original relaxation oscillation frequency of the laser. A large microwave frequency range of a few to over 100 GHz is achievable by simply adjusting the optical injection parameters;
- (3) Frequency Modulation Capability: For a fixed master-slave detuning frequency f_i , the generated microwave frequency f_o would increase approximately linearly with the injection strength ζ_i over a large range, which has been verified in Figure 4b. This unique feature provides a convenient way to flexibly control the instantaneous frequency of the generated microwave signal. Therefore, assisted by dynamical modulation of injection parameters, wideband reconfigurable microwave frequency-modulated signals can be generated, which has important applications in modern communication and radar systems.

3. Photonic Microwave Stabilization for P1 Dynamics

Despite the above advantages, the generated microwave signal based on the P1 dynamics of an OISL has poor spectral purity and limited frequency stability, which hampers its usefulness to many practical applications. On the one hand, the generated microwave signal has a relatively large 3-dB microwave linewidth, typically on the order of 1–10 MHz, which mainly arises from the spontaneous emission noise of the injected laser. On the other hand, fluctuations in the optical injection frequency and power result in significant microwave frequency jitters, typically on the order of 10–100 MHz. To cope with these problems, several photonic microwave stabilization approaches for P1 nonlinear dynamics have been proposed, which can be classified into two main categories, i.e., microwave modulation stabilization, and delayed feedback stabilization [27–36].

3.1. Microwave Modulation Stabilization

Figure 5 shows two typical configurations of photonic microwave stabilization for P1 dynamics using microwave modulation. As shown in Figure 5a, on the basis of the conventional optical injection system, an external microwave signal with a frequency f_L from a microwave frequency synthesizer (MFS) is applied to directly modulate the injected SL. By properly setting the frequency and power of the microwave modulation signal, the microwave signal generated by P1 oscillation could be locked to the MFS, thus improving the spectral purity and frequency stability. Simpson et al. demonstrated that the microwave linewidth can be reduced to below 1 kHz, when the MFS frequency was tuned to the P1 frequency, namely, $f_L = f_o$ [27]. This method, also known as optical double-locking, has limitations in generating high-frequency microwave signals: (1) high-frequency modulation is difficult due to the limited laser response of direct modulation; (2) a stable microwave

signal with the same frequency as the P1 oscillation frequency is needed. In [27], the highest locked microwave frequency was limited to approximately 17 GHz.

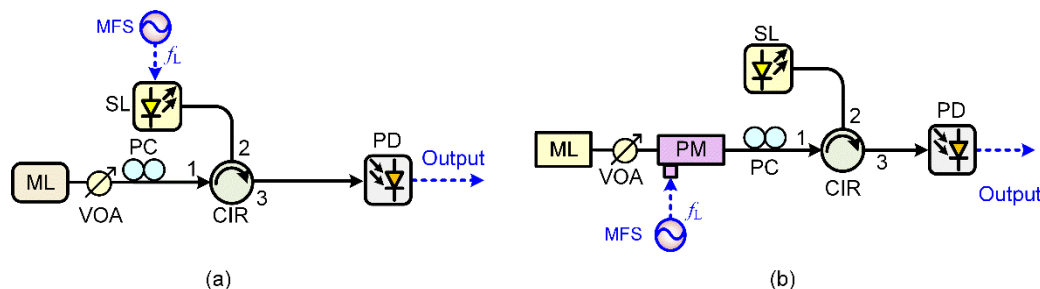


Figure 5. Photonic microwave stabilization for P1 dynamics using microwave modulation. (a) Direct microwave modulation; (b) optical modulation sideband injection locking. MS: microwave frequency synthesizer; PM: phase modulator.

To address the above problems, Fan et al. proposed a subharmonic microwave modulation stabilization scheme [28,29], i.e., an MFS with a frequency of $f_L \approx f_o/N$ (N is an integer larger than one) is employed to modulate the SL. With a proper modulation power, the modulation sidebands around the injection light at $f_m \pm Nf_L$ and P1 oscillation sidebands at $f_m \pm f_o$ become mutually locked. Consequently, the P1 oscillation is stabilized, while the P1 frequency f_o is locked and driven to Nf_L . In the experimental demonstration, via 1/4 and 1/9 subharmonic microwave modulation, a stabilized microwave signal up to 65.07 GHz was obtained with a linewidth below 1.6 kHz and a single-sideband (SSB) phase noise less than -98 dBc/Hz at 10 kHz [29]. Figure 5b presents a schematic diagram of the optical modulation sideband injection-locking approach. A high-purity microwave signal (f_L) is used to drive an optical phase modulator (PM), which has a larger modulation bandwidth than the SL. After PM, the injection signal from ML carrying multiple modulation sidebands is injected into the SL and injection-locks the P1 oscillation when f_L is approximately equal to f_o/N (N is a positive integer). As a result, the poor microwave spectral purity and limited stability of the P1 oscillation state are effectively improved to a level close to that of the microwave reference. In [30], Hung et al. reported that the 3-dB linewidth was reduced to less than 1 Hz for microwave generation up to 40 GHz. Recently, V- and W-band microwave signal generation has been realized based on a similar setup in Figure 5b [31]. Furthermore, cascaded injection of semiconductor lasers in P1 oscillations has also been investigated for stabilized signal generation in the millimeter-wave range [32].

3.2. Delayed Feedback Stabilization

To eliminate the requirement of a high-performance microwave reference signal, photonic microwave stabilization methods for P1 dynamics using a delayed feedback loop were proposed [33–36]. Figure 6a is a schematic diagram of the optical feedback stabilization approach. In this scheme, a portion of the output optical signal from the optical circulator, which carries a microwave modulation with a frequency of f_o is fed back to inject the SL and locks the P1 oscillation. An optical tunable delay-line (OTDL) and a variable optical attenuator (VOA2) are inserted in the feedback loop to optimize the feedback delay and feedback strength. In other words, the optical injection is responsible for the generation of the modulated optical signal through the P1 oscillation dynamics, and the optical feedback loop provides the delayed replica of the optical signal to injection-lock itself to stabilize the P1 oscillation. In [33], Zhuang et al. demonstrated the generation of 45.424 GHz signal with a linewidth less than 50 kHz using the optical feedback stabilization of P1 oscillation dynamics. However, it is difficult to further reduce the obtained linewidth of generated microwave signal, which is influenced by the optical interference between the original injection signal and the delayed feedback signal. In [34], Simpson et al. reported that using a polarization-rotated feedback loop can reduce the impact of the optical interference noise,

and the linewidth of the P1 oscillation signal was narrowed to ~3 kHz. The main drawback of this method is that the polarization of the feedback signal should be carefully aligned.

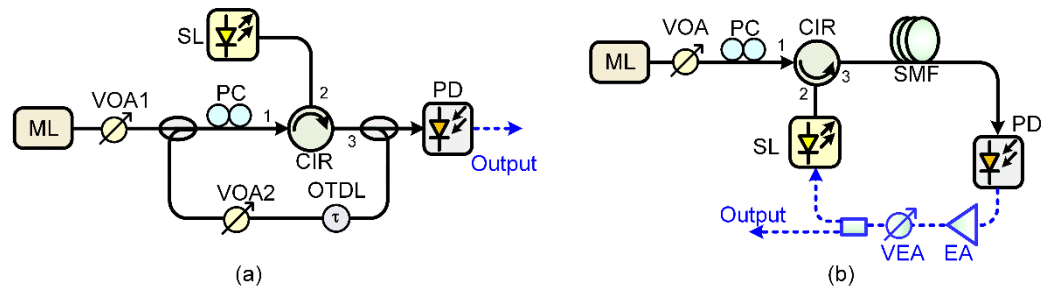


Figure 6. Photonic microwave stabilization for P1 dynamics using a delayed feedback cavity. (a) Optical feedback stabilization; (b) optoelectronic feedback stabilization. OTDL: optical tunable delay-line; SMF: single-mode fiber; VEA: variable electrical attenuator; EA: electrical amplifier.

Compared with the optical feedback stabilization scheme, the optoelectronic feedback stabilization scheme is more favorable to overcome the influence of optical interference, as shown in Figure 6b. Instead of using an MFS in Figure 5a, the delayed replica of the generated microwave signal by P1 oscillation is employed to modulate the SL and stabilize the P1 oscillation after passing through a proper delay and power adjustment. The principle of this method can also be understood to be that the P1 oscillation signal is spectrally filtered by the high-Q external feedback cavity. The linewidth was reduced to the range of 10–160 kHz for the P1 frequency in the range 10–23 GHz with stabilization through a 10 m optoelectronic feedback cavity [35]. Afterwards, Suelzer et al. demonstrated that a linewidth below 3 Hz and an SSB phase noise below -95 dBc/Hz at 10 kHz were achieved with dual-loop optoelectronic feedback of 10 km and 10.1 km, respectively [36]. The aim of adopting a dual-loop structure in the delayed feedback stabilization approach is to suppress the undesired side modes based on the Vernier effect [37].

For the schemes in Figure 6b, the fiber and other devices in the feedback cavity are sensitive to environmental perturbations. Therefore, the frequency accuracy and stability of the generated microwave signal are limited. In addition, the phase noise performance at low offset frequencies deteriorates. In [38], Zhou et al. proposed combining the advantages of subharmonic microwave modulation and dual-loop optoelectronic feedback to stabilize the P1 oscillation signal of OISLs, as shown in Figure 7. Therefore, both the performance of the spectral purity and frequency stability were significantly improved. As shown in Figure 8a,b, a 17.45 GHz signal was generated with a side-mode suppression ratio of 70.08 dB and an SSB phase noise of -87.13 (-113.39) dBc/Hz at 1 kHz (10 kHz). Furthermore, the frequency drift over a period of 20 min, which characterizes the long-term stability, was reduced to less than 1 Hz, as shown in Figure 8c.

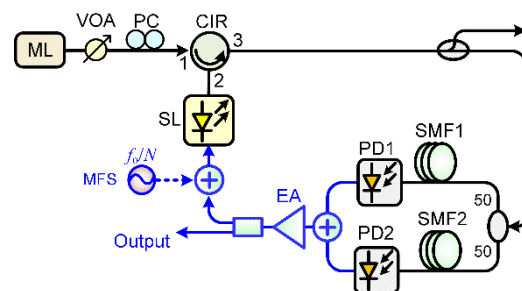


Figure 7. Photonic microwave stabilization for P1 dynamics using subharmonic microwave modulation and dual-loop optoelectronic feedback.

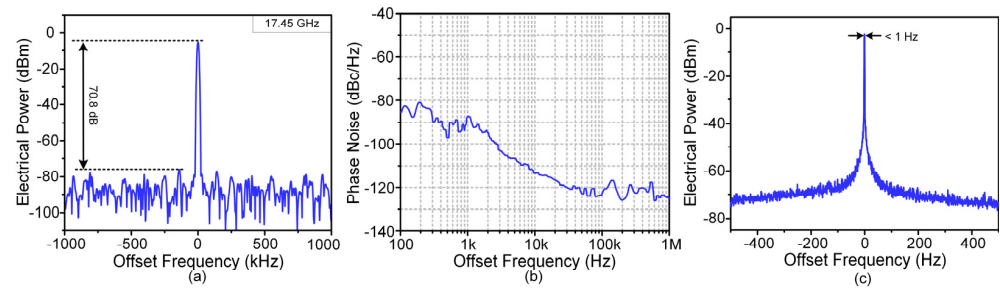


Figure 8. The results of the stabilized 17.45 GHz signal [38]. (a) Electrical spectrum; (b) traces of microwave frequency drifts in 20 min; (c) SSB phase noise spectrum.

4. Photonic Microwave Applications Based on P1 Dynamics

As mentioned in Section 3, photonic microwave generation using the P1 oscillation of an OISL has some unique advantages. In recent years, various potential applications of P1 dynamics-based microwave signal generators in the field of microwave photonics have been reported. On the one hand, diverse signal generation has been implemented based on P1 dynamics, including the following: linear frequency-modulated (LFM) microwave waveforms, microwave frequency combs (MFCs), and chaotic signals. In addition, microwave frequency conversion, optical DSB-to-SSB conversion, photonic microwave carrier recovery and other photonics microwave signal processing schemes have also been presented.

4.1. Diverse Signal Generation

A linear frequency-modulated (LFM) microwave waveform with a large time-bandwidth product (TBWP) is one of the most widely used transmitting waveforms in modern radar systems to simultaneously achieve a large detection range and a high ranging resolution. Numerous photonic approaches have been proposed to generate LFM waveforms, including the space-to-time mapping method [39,40], spectral shaping and frequency-to-time mapping method [41], external phase modulation method [42,43], and self-heterodyne method [44]. LFM waveform generation can also be realized based on the P1 oscillation of an OISL [45]. Compared with these photonic schemes using a spatial light modulator, fabricated fiber Bragg grating (FBG), femtosecond pulsed laser, high-speed modulator, high-speed electrical arbitrary waveform generator (AWG) or specially designed wavelength sweeping laser, the P1 oscillation-based approach only needs a commercial semiconductor laser and a low-speed intensity modulator. In addition, it has the advantages of a large TBWP and high tunability. As shown in Figure 9, an “injection strength controller”, which consists of an intensity modulator (IM) and an electrical control signal $S(t)$, is inserted into the optical injection system to dynamically control the optical injection ζ_i and the resultant P1 frequency f_o . Through setting $S(t)$ to have a near-sawtooth profile, the optical injection strength and the resultant output microwave frequency increase linearly, namely, an LFM waveform is obtained. In addition, the main operating parameters of the generated LFM signal are tunable by adjusting the injection parameters and/or the control signal, including the center frequency, bandwidth, and temporal period.

Figure 10 gives an example of the generated LFM waveform. Figure 10a is a 1 MHz control signal, and its profile is designed to compensate for the nonlinearity of the amplitude transfer function of the system [45,46]. As seen from Figure 10b,c, an LFM signal centered at 16 GHz with a bandwidth of 12 GHz and a temporal period of 1 μ s was generated, leading to a large TBWP of 1.2×10^4 . In addition to the LFM signal, the P1 oscillation state of an optically injected semiconductor laser has been applied to the generation of other radar waveforms, such as microwave frequency-hopping sequences, nonlinear frequency-modulated (NLFM) waveforms, and dual-chirp LFM waveforms [47–49]. Similar to Section 3.2, the spectral purity and stability of the generated LFM signals based on the P1 oscillation of an OISL can be improved using delayed feedback stabilization approaches,

including optoelectronic feedback stabilization [50,51] and optical feedback stabilization approaches [52]. Recently, another generation approach based on P1 laser dynamics of an OISL has been demonstrated for LFM signal generation [53]. The optical modulation sideband injection-locking structure in Figure 5b is adopted, and the MFS is replaced by an AWG to vary the modulation frequency. Through the phase locking established between the modulated optical injection and the P1 oscillation signal, LFM signals with high stability and purity are achieved.

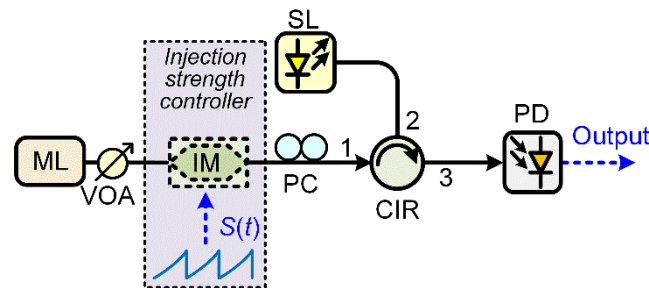


Figure 9. Schematic diagram of the LFM waveform generator. IM: intensity modulator.

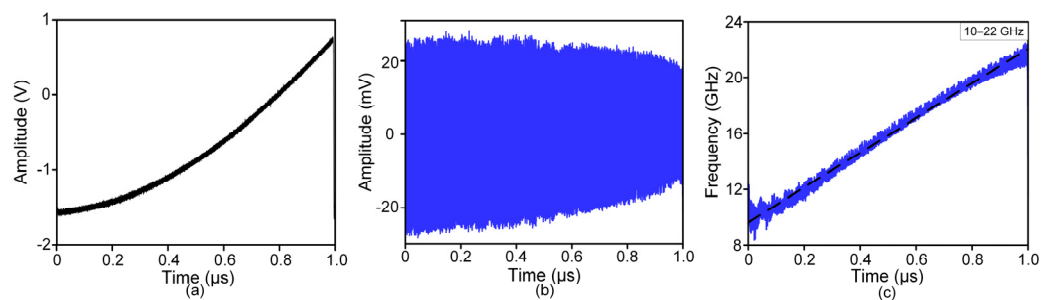


Figure 10. Results of the generated LFM waveform [45]. (a) Control signal $S(t)$; (b) temporal waveform; (c) the recovered instantaneous frequency.

Microwave frequency comb (MFC) signals, which consist of a series of uniformly spaced frequency components with a coherent and stable phase relationship, are highly attractive for various applications, including radar detection, radio-over-fiber systems, and metrology. A typical photonics-based MFC generation approach is heterodyning an optical frequency comb (OFC) from an MLL. However, the comb spacing of the generated MFC signals has poor tunability due to the limited pulse repetition rate of the MLL [54]. Alternatively, photonic MFC generation can be realized by P1 oscillation of an OISL. In [55], Fan et al. reported that the generation of broadband MFC signals can be realized based on the same setup in Figure 5a. First, the OISL was driven into the P1 state with a fundamental frequency of $f_o = 26.44$ GHz. Then, by adopting a 1/8 subharmonic modulation with a proper modulation power, an MFC with a bandwidth of 59.4 GHz within a 10 dB flatness was experimentally obtained, and the comb spacing was equal to $f_L = 3.3$ GHz. Dense MFC signals, which have a small comb spacing, can also be produced based on the P1 oscillation of an OISL. In [56], Zhang et al. utilized an OISL with dual-loop optoelectronic feedback for generating high-performance dense MFC signals. A sinusoidal voltage signal is used to modulate the P1 oscillation of the OISL for the initial MFC generation, and then two optoelectronic feedback loops are introduced to enhance the performance of the MFC: a short-delay feedback loop is first applied to improve comb contrast based on Fourier domain mode locking (FDML), and a long-delay feedback loop is added to reduce the comb linewidth based on the self-injection-locking technique. As shown in Figure 11, a K-band MFC (18–26 GHz) with a line spacing of 8.45 MHz was obtained, where a comb linewidth of approximately 500 Hz and a comb contrast over 45 dB were simultaneously achieved.

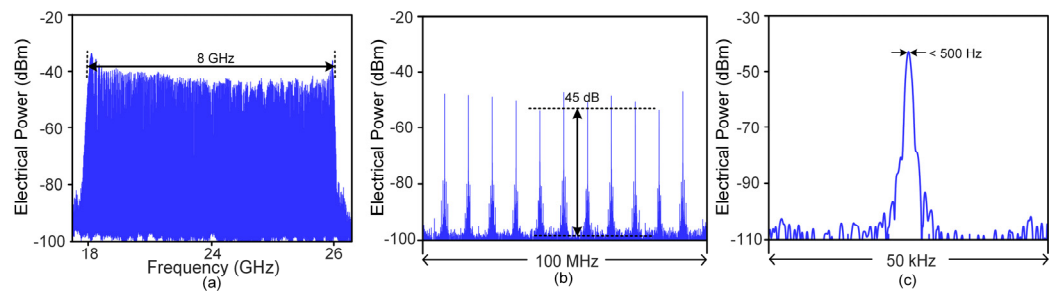


Figure 11. Electrical spectra of the generated dense MFC signals [56]. (a) Span: 9 GHz, RBW: 10 kHz; (b) Span: 100 MHz, RBW: 6.25 kHz; (c) Span: 50 kHz, RBW: 500 Hz.

The P1 oscillation of an OISL can also be applied for the generation of broadband chaotic signals. Through destabilization of P1 nonlinear dynamics in a semiconductor laser subject to intensity-modulated optical injection, Tseng et al. experimentally generated chaotic microwaves with a bandwidth of approximately 33 GHz, which is much wider than that generated by the chaotic oscillation state of an OISL [57]. A numerical study has also been conducted to systematically investigate this approach in wider regions of injection and modulation parameters [58]. The results proved that intensity-modulated optical injection is able to obtain chaotic signals in wider parameter regions in contrast with the case of optical injection alone. Recently, broadband chaos generation with record-high entropy has been demonstrated using the same approach, which can be used as a 2-bit physical random number generator at a rate of 160 Gbits/s [59].

4.2. Photonic Microwave Signal Processing

P1 nonlinear dynamics can also find applications in photonic microwave signal processing. Microwave frequency multipliers facilitate frequency multiplication from a low-frequency input signal (f_{IN}) to a high-frequency output signal (f_{OUT}), described as $f_{OUT} = N f_{IN}$ (N is an integer larger than one). In fact, the photonic microwave stabilization scheme for P1 dynamics using microwave modulation in Figure 5 can function as a microwave frequency multiplier, which also satisfies the aforementioned frequency relationship [28,29,60]. Since an OISL operating at the P1 state is by itself a photonic microwave oscillator with a broad tuning range, it can be used as the local oscillator (LO) signal in a microwave photonic frequency mixer. Both microwave frequency up-conversion and down-conversion have been realized based on the P1 dynamics of an OISL [61,62]. Furthermore, taking advantage of subharmonic modulation stabilization of P1 dynamics, Zhou et al. demonstrated a photonic microwave harmonic down-converter based on an OISL, which can essentially lower the demand for the LO frequency in the frequency mixer, as shown in Figure 12a [63]. In the experiment, the 4th, 6th, 9th, and 12th harmonic down-conversions were demonstrated, and an RF signal with a frequency as high as 39 GHz was down-converted to frequency-tunable intermediate frequency (IF) signals within 2 GHz. Figure 12b,c display the optical spectrum before photodetection and the electrical spectrum of the 1.4-GHz IF signal for the 4th harmonic down-conversion. Previously, major photonic microwave harmonic down-conversion methods have been reported based on OFCs or MLLs [64,65]. The main drawbacks lie in the limited tunability and complex structures, i.e., consisting of multiple electro-optic modulators or semiconductor optical amplifiers. As a comparison, the proposed photonic MHDC features a wide frequency range, flexible harmonic factors, a low LO-frequency, and a simple structure.

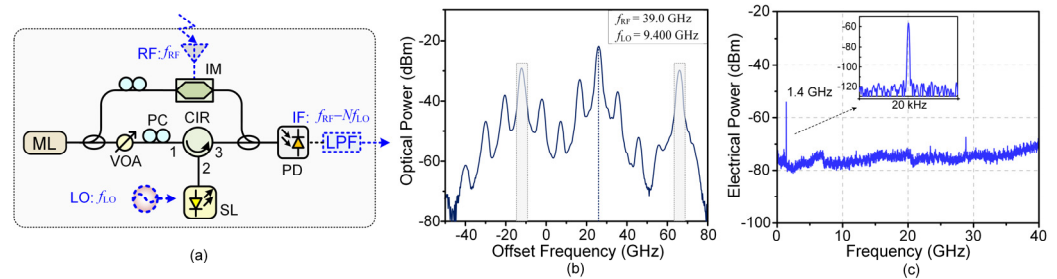


Figure 12. (a) Schematic of the photonic microwave harmonic down-converter; LPF: low-pass filter; (b) optical spectrum before photodetection; (c) electrical spectrum of the 1.4-GHz IF signal [63].

As mentioned in Section 2, the optical spectrum of an OISL operating at P1 dynamics consists of highly intensity-asymmetric sidebands separated from the regeneration of the injection by the P1 oscillation frequency f_o . The high asymmetry in the optical power of the oscillation sidebands is due to the redshifting effect. Based on these unique characteristics, P1 dynamics have been studied for applications of optical DSB modulation to SSB modulation conversion, and photonic microwave carrier recovery [66,67]. In [66], Hung et al. experimentally demonstrated optical DSB-to-SSB conversion by taking advantage of oscillation sideband asymmetry. An optical DSB signal with modulation frequency up to 40 GHz was successfully converted to an optical SSB signal with an intensity difference of over 20 dB. An all-optical microwave carrier recovery scheme based on P1 nonlinear dynamics of an OISL for coherent detection in an orthogonal frequency division multiplexing radio-over-fiber (OFDM-RoF) link was demonstrated [67]. Through the injection locking established between the OFDM-RoF signal and the P1 dynamics, the recovered microwave carrier inherently possesses the same frequency and preserved phase quality as those of the original microwave carrier. A bit-error ratio (BER) as low as 1.9×10^{-9} was experimentally achieved using the proposed scheme for coherent detection of a 32-GHz OFDM-RoF signal with 4 Gb/s 16-quadrature amplitude modulation (QAM) [67].

5. Discussion and Conclusions

In conclusion, we reviewed recent advances in P1 dynamics-based tunable microwave signal generation techniques. Two typical approaches to stabilize the P1 oscillation and thus improve the spectral purity and stability of the generated microwave signal are introduced, i.e., microwave modulation stabilization, and delayed feedback stabilization. Applications of P1 dynamics of an OISL in diverse signal generation and photonic microwave signal processing, were also described, including the following: LFM waveform generation, MFC generation, chaotic signal generation, microwave frequency conversion, optical DSB-to-SSB conversion, and photonic microwave carrier recovery. It should be noted that other potential applications of the P1 dynamics-based microwave signal generator have also been reported, such as triangular waveform generation [68], optical pulse generation [69], photonic microwave signal amplification [70], photonic microwave time delay [71], microwave frequency measurement [72], and lidar and radar systems [73,74], which are not discussed in this paper.

Currently, photonic microwave generation and applications based on P1 dynamics are mainly realized using commercial semiconductor lasers, e.g., distributed feedback (DFB) lasers and vertical-cavity surface-emitting lasers (VCSELs). In the future, more research should be devoted to controlling the P1 dynamics of new lasers for photonic microwave generation and applications, which may have a simpler structure and higher performance [75–77]. One possible laser is spin-polarized VCSEL (spin-VCSEL), which can be utilized for broad tunable photonic microwave generation, and no additional master laser is needed [77]. In addition, taking advantage of integrated microwave photonic technologies [78], an on-chip optical injection system is possible, which is expected to achieve better performance for practical applications.

Author Contributions: Resources and review, P.Z.; project administration and supervision, S.P. and N.L.; All authors contributed to the data analysis and manuscript writing. All authors have read and agreed to the published version of the manuscript.

Funding: This research was funded by the National Natural Science Foundation of China, grant numbers 62001317, 62004135, 62004135; the Natural Science Foundation of Jiangsu Province, grant number BK20200855; the Natural Science Research Project of Jiangsu Higher Education Institutions of China, grant numbers 20KJB510011, 20KJA416001; and the Project of Key Laboratory of Radar Imaging and Microwave Photonics (Nanjing University of Aeronautics and Astronautics), Ministry of Education, grant numbers RIMP2020001.

Informed Consent Statement: Not applicable.

Data Availability Statement: Data underlying the results presented in this paper are not publicly available at this time but may be obtained from the authors upon reasonable request.

Conflicts of Interest: The authors declare no conflict of interest.

References

1. Ghelfi, P.; Laghezza, F.; Scotti, F.; Serafino, G.; Capria, A.; Pinna, S.; Onori, D.; Porzi, C.; Scaffardi, M.; Malacarne, A. A fully photonics-based coherent radar system. *Nature* **2014**, *507*, 341–345. [PubMed]
2. Pan, S.L.; Zhu, D.; Liu, S.F.; Xu, K.; Dai, Y.T.; Wang, T.L.; Liu, J.G.; Zhu, N.H.; Xue, Y.; Liu, N.J. Satellite payloads pay off. *IEEE Microw. Mag.* **2015**, *16*, 61–73.
3. Pan, S.L.; Zhang, Y.M. Microwave photonic radars. *J. Lightwave Technol.* **2020**, *38*, 5450–5484.
4. Kittlaus, E.A.; Eliyahu, D.; Ganji, S.; Williams, S.; Matsko, A.B.; Cooper, K.B.; Forouhar, S. A low-noise photonic heterodyne synthesizer and its application to millimeter-wave radar. *Nat. Commun.* **2021**, *12*, 4397.
5. Zhang, Y.M.; Zhang, F.Z.; Pan, S.L. Generation of frequency-multiplied and phase-coded signal using an optical polarization division multiplexing modulator. *IEEE Trans. Microw. Theory Tech.* **2017**, *65*, 651–660.
6. Pillet, G.; Morvan, L.; Brunel, M.; Bretenaker, F.; Dolfi, D.; Vallet, M.; Huignard, J.P.; Floch, A.L. Dual-frequency laser at 1.5 μm for optical distribution and generation of high-purity microwave signals. *J. Lightwave Technol.* **2008**, *26*, 2764–2773.
7. Xie, X.P.; Bouchand, R.; Nicolodi, D.; Giunta, M.; Haensel, W.; Lezius, M.; Joshi, A.; Datta, S.; Alexandre, C.; Lours, M.; et al. Photonic microwave signals with zeptosecond level absolute timing noise. *Nat. Photonics* **2017**, *44*, 44–47.
8. Maleki, L. The optoelectronic oscillator. *Nat. Photonics* **2011**, *5*, 728–730.
9. Simpson, T.B.; Liu, J.M. Enhanced modulation bandwidth in injection-locked semiconductor lasers. *IEEE Photon. Technol. Lett.* **1997**, *9*, 1322–1324.
10. Hwang, S.K.; Liang, D.H. Effects of linewidth enhancement factor on period-one oscillations of optically injected semiconductor lasers. *Appl. Phys. Lett.* **2006**, *89*, 061120.
11. Lee, C.H.; Shin, S.Y. Self-pulsing, spectral bistability, and chaos in a semiconductor laser diode with optoelectronic feedback. *Appl. Phys. Lett.* **1993**, *62*, 922–924.
12. Tang, S.; Liu, J.M. Chaotic pulsing and quasi-periodic route to chaos in a semiconductor laser with delayed opto-electronic feedback. *IEEE J. Quantum Electron.* **2001**, *37*, 329–336.
13. Lin, F.Y.; Liu, J.M. Harmonic frequency locking in a semiconductor laser with delayed negative optoelectronic feedback. *Appl. Phys. Lett.* **2002**, *81*, 3128–3130.
14. Kovanis, V.; Gavrielides, A.; Simpson, T.B.; Liu, J.M. Instabilities and chaos in optically injected semiconductor lasers. *Appl. Phys. Lett.* **1995**, *67*, 2780–2782.
15. Lin, F.Y.; Liu, J.M. Diverse waveform generation using semiconductor lasers for radar and microwave applications. *IEEE J. Quantum Electron.* **2004**, *40*, 682–689.
16. Simpson, T.B.; Liu, J.M.; Gavrielides, A. Bandwidth enhancement and broadband noise reduction in injection-locked semiconductor lasers. *IEEE Photon. Technol. Lett.* **1995**, *7*, 709–711.
17. Jiang, P.; Zhou, P.; Li, N.Q.; Mu, P.H.; Li, X.F. Optically injected nanolasers for time-delay signature suppression and communications. *Opt. Express.* **2020**, *28*, 26421–26435.
18. Uchida, A.; Amano, K.; Inoue, M.; Hirano, K.; Naito, S.; Someya, H.; Oowada, I.; Kurashige, T.; Shiki, M.; Yoshimori, S.; et al. Fast physical random bit generation with chaotic semiconductor lasers. *Nat. Photonics* **2008**, *2*, 728–732.
19. Lin, F.Y.; Liu, J.M. Chaotic lidar. *IEEE J. Sel. Top. Quantum Electron.* **2004**, *10*, 991–997.
20. Chan, S.C. Analysis of an optically injected semiconductor laser for microwave generation. *IEEE J. Quantum Electron.* **2010**, *46*, 421–428.
21. Hwang, S.K.; Liu, J.M.; White, J.K. Characteristics of period-one oscillations in semiconductor lasers subject to optical injection. *IEEE J. Sel. Top. Quantum Electron.* **2004**, *10*, 974–981.
22. Simpson, T.B.; Liu, J.M.; Huang, K.F.; Tai, K. Nonlinear dynamics induced by external optical injection in semiconductor lasers. *Quantum Semiclass. Opt.* **1997**, *9*, 765–784.

23. Zhuang, J.P.; Chan, S.C. Phase noise characteristics of microwave signals generated by semiconductor laser dynamics. *Opt. Express*. **2015**, *23*, 2777–2797. [[PubMed](#)]
24. Hwang, S.K.; Liu, J.M. Dynamical characteristics of an optically injected semiconductor laser. *Opt. Commun.* **2000**, *183*, 195–205.
25. Chan, S.C.; Hwang, S.K.; Liu, J.M. Radio-over-fiber AM-to-FM upconversion using an optically injected semiconductor laser. *Opt. Lett.* **2006**, *31*, 2254–2256. [[PubMed](#)]
26. Zhou, P.; Zhang, F.Z.; Guo, Q.S.; Li, S.M.; Pan, S.L. Reconfigurable radar waveform generation based on an optically injected semiconductor laser. *IEEE J. Sel. Top. Quantum Electron.* **2017**, *23*, 1801109.
27. Simpson, T.B.; Doft, F. Double-Locked Laser Diode for Microwave Photonics Applications. *IEEE Photon. Technol. Lett.* **1999**, *11*, 1476–1478.
28. Fan, L.; Wu, Z.M.; Deng, T.; Wu, J.G.; Tang, X.; Chen, J.J.; Mao, S.; Xia, G.Q. Subharmonic microwave modulation stabilization of tunable photonic microwave generated by period-one nonlinear dynamics of an optically injected semiconductor laser. *J. Lightwave Technol.* **2014**, *32*, 4058–4064.
29. Fan, L.; Xia, G.Q.; Chen, J.J.; Tang, X.; Liang, Q.; Wu, Z.M. High-purity 60 GHz band millimeter-wave generation based on optically injected semiconductor laser under subharmonic microwave modulation. *Opt. Express* **2016**, *24*, 18252–18265.
30. Hung, Y.H.; Hwang, S.K. Photonic microwave stabilization for period-one nonlinear dynamics of semiconductor lasers using optical modulation sideband injection locking. *Opt. Express* **2015**, *23*, 6520–6532.
31. Tseng, C.H.; Lin, C.T.; Hwang, S.K. V- and W-band microwave generation and modulation using semiconductor lasers at period-one nonlinear dynamics. *Opt. Lett.* **2020**, *45*, 6819–6822. [[PubMed](#)]
32. Zhang, L.; Chan, S.C. Cascade injection of semiconductor lasers in period-one oscillations for millimeter-wave generation. *Opt. Lett.* **2019**, *44*, 4905–4908. [[PubMed](#)]
33. Zhuang, J.P.; Chan, S.C. Tunable photonic microwave generation using optically injected semiconductor laser dynamics with optical feedback stabilization. *Opt. Lett.* **2013**, *38*, 344–346. [[PubMed](#)]
34. Simpson, T.B.; Liu, J.M.; Almulla, M.; Usechak, N.G.; Kovanis, V. Linewidth sharpening via polarization-rotated feedback in optically injected semiconductor laser oscillators. *IEEE J. Sel. Top. Quantum Electron.* **2013**, *19*, 1500807.
35. Chan, S.C.; Liu, J.M. Tunable narrow-linewidth photonic microwave generation using semiconductor laser dynamics. *IEEE J. Sel. Top. Quantum Electron.* **2004**, *10*, 1025–1032.
36. Suelzer, J.S.; Simpson, T.B.; Devgan, P.; Usechak, N.G. Tunable, low-phase-noise microwave signals from an optically injected semiconductor laser with opto-electronic feedback. *Opt. Lett.* **2017**, *42*, 3181–3184.
37. Yao, X.S.; Maleki, L. Multiloop optoelectronic oscillator. *IEEE J. Quantum Electron.* **2000**, *36*, 79–84.
38. Zhou, P.; Zhang, F.Z.; Zhang, D.C.; Pan, S.L. Performance enhancement of an optically-injected-semiconductor-laser-based optoelectronic oscillator by subharmonic microwave modulation. *Opt. Lett.* **2018**, *43*, 5439–5442.
39. McKinney, J.D.; Leaird, D.E.; Weiner, A.M. Millimeter-wave arbitrary waveform generation with a direct space-to-time pulse shaper. *Opt. Lett.* **2002**, *27*, 1345–1347.
40. Li, M.; Wang, C.; Li, W.Z.; Yao, J.P. An unbalanced temporal pulse-shaping system for chirped microwave waveform generation. *IEEE Trans. Microw. Theory Tech.* **2010**, *58*, 2968–2975.
41. Wang, C.; Yao, J.P. Photonic generation of chirped microwave pulses using superimposed chirped fiber Bragg gratings. *IEEE Photon. Technol. Lett.* **2008**, *20*, 882–884.
42. Li, W.Z.; Yao, J.P. Generation of linearly chirped microwave waveform with an increased time-bandwidth product based on a tunable optoelectronic oscillator and a recirculating phase modulation loop. *J. Lightwave Technol.* **2014**, *32*, 3573–3579.
43. Brunetti, G.; Marocco, G.; Armenise, M.N.; Ciminelli, C. High performance chirped microwave generator for space applications. In Proceedings of the 2020 International Conference on Space Optics (ICSO 2020), Online, 30 March–2 April 2020; pp. 1230–1239.
44. Coutinho, O.L.; Zhang, J.J.; Yao, J.P. Photonic generation of a linearly chirped microwave waveform with a large time-bandwidth product based on self-heterodyne technique. In Proceedings of the 2015 International Topical Meeting on Microwave Photonics (MWP 2015), Paphos, Cyprus, 26–29 October 2015.
45. Zhou, P.; Zhang, F.Z.; Guo, Q.S.; Pan, S.L. Linearly chirped microwave waveform generation with large time-bandwidth product by optically injected semiconductor laser. *Opt. Express* **2016**, *24*, 18460–18467. [[PubMed](#)]
46. Zhang, B.W.; Zhu, D.; Zhou, P.; Xie, C.X.; Pan, S.L. Tunable triangular frequency modulated microwave waveform generation with improved linearity using an optically injected semiconductor laser. *Appl. Opt.* **2019**, *58*, 5479–5485.
47. Zhou, P.; Zhang, F.Z.; Ye, X.W.; Guo, Q.S.; Pan, S.L. Flexible frequency-hopping microwave generation by dynamic control of optically injected semiconductor laser. *IEEE Photon. J.* **2016**, *8*, 5501909.
48. Zhou, P.; Zhang, R.H.; Li, K.X.; Jiang, Z.D.; Mu, P.H.; Bao, H.L.; Li, N.Q. Generation of NLFM microwave waveforms based on controlled period-one dynamics of semiconductor lasers. *Opt. Express* **2020**, *28*, 32647–32656.
49. Zhou, P.; Chen, H.; Li, N.Q.; Zhang, R.H.; Pan, S.L. Photonic generation of tunable dual-chirp microwave waveforms using a dual-beam optically injected semiconductor laser. *Opt. Lett.* **2020**, *45*, 1342–1345.
50. Zhuang, J.P.; Li, X.Z.; Li, S.S.; Chan, S.C. Frequency-modulated microwave generation with feedback stabilization using an optically injected semiconductor laser. *Opt. Lett.* **2016**, *41*, 5764–5767.
51. Zhou, P.; Zhang, F.Z.; Pan, S.L. Generation of linear frequency-modulated waveforms by a frequency-sweeping optoelectronic oscillator. *J. Lightwave Technol.* **2018**, *36*, 3927–3934.

52. Lin, X.D.; Xia, G.Q.; Shang, Z.; Deng, T.; Tang, X.; Fan, L.; Gao, Z.Y.; Wu, Z.M. Frequency-modulated continuous-wave generation based on an optically injected semiconductor laser with optical feedback stabilization. *Opt. Express* **2019**, *27*, 1217–1225.
53. Tseng, C.H.; Hung, Y.H.; Hwang, S.K. Frequency-modulated continuous-wave microwave generation using stabilized period-one nonlinear dynamics of semiconductor lasers. *Opt. Lett.* **2019**, *44*, 3334–3337. [[PubMed](#)]
54. Hagmann, M.J.; Stenger, F.S.; Yarotski, D.A. Linewidth of the harmonics in a microwave frequency comb generated by focusing a mode-locked ultrafast laser on a tunneling junction. *J. Appl. Phys.* **2013**, *114*, 223107.
55. Li, Y.H.; Xia, G.Q.; Wu, Z.M. Tunable and broadband microwave frequency comb generation using optically injected semiconductor laser nonlinear dynamics. *IEEE Photon. J.* **2017**, *9*, 5502607.
56. Zhang, R.H.; Zhou, P.; Li, K.X.; Bao, H.L.; Li, N.Q. Photonic generation of high-performance microwave frequency combs using an optically injected semiconductor laser with dual-loop optoelectronic feedback. *Opt. Lett.* **2021**, *46*, 4622–4625. [[PubMed](#)]
57. Tseng, C.H.; Hwang, S.K. Broadband chaotic microwave generation through destabilization of period-one nonlinear dynamics in semiconductor lasers for radar applications. *Opt. Lett.* **2020**, *45*, 3777–3780.
58. Zeng, Y.; Zhou, P.; Huang, Y.; Li, N.Q. Optical chaos generated in semiconductor lasers with intensity-modulated optical injection: A numerical study. *Appl. Opt.* **2021**, *60*, 7963–7972.
59. Tseng, C.H.; Funabashi, R.; Kanno, K.; Uchida, A.; Wei, C.C.; Hwang, S.K. High-entropy chaos generation using semiconductor lasers subject to intensity-modulated optical injection for certified physical random number generation. *Opt. Lett.* **2021**, *46*, 3384–3387.
60. Chen, H.; Ukaegbu, I.; Nakarmi, B.; Pan, S.L. RF multiplier based on harmonic-locked SMFP-LD and OEO structure. *IEEE Access* **2022**, *10*, 435–440.
61. Hung, Y.H.; Hwang, S.K. Highly efficient local-oscillator-free photonic microwave down-converters based on period-one nonlinear dynamics of semiconductor lasers. In Proceedings of the SPIE Photonics West Conference, San Francisco, CA, USA, 13–18 February 2016; p. 974718.
62. Han, B.C.; Yu, J.L.; Wang, W.R. Local oscillator free all optical OOK signal frequency up conversion enabled by injection locking of Fabry-Pérot laser. *Opt. Commun.* **2014**, *325*, 40–46.
63. Zhou, P.; Li, N.Q.; Pan, S.L. Photonic microwave harmonic down-converter based on stabilized period-one nonlinear dynamics of semiconductor lasers. *Opt. Lett.* **2019**, *44*, 4869–4872.
64. Ghelfi, P.; Serafino, G.; Scotti, F.; Laghezza, F.; Bogoni, A. Flexible receiver for multiband orthogonal frequency division multiplexing signals at the millimeter waveband based on optical downconversion. *Opt. Lett.* **2012**, *37*, 3924–3926. [[PubMed](#)]
65. Zou, X.H.; Zhang, S.J.; Wang, H.; Zhang, Z.Y.; Li, J.J.; Zhang, Y.L.; Liu, S.; Liu, Y. Microwave photonic harmonic down-conversion based on cascaded four-wave mixing in a semiconductor optical amplifier. *IEEE Photon. J.* **2018**, *10*, 5500308.
66. Hung, Y.H.; Chu, C.H.; Hwang, S.K. Optical double-sideband modulation to single-sideband modulation conversion using period-one nonlinear dynamics of semiconductor lasers for radio-over-fiber links. *Opt. Lett.* **2013**, *38*, 1482–1484. [[PubMed](#)]
67. Hung, Y.H.; Yan, J.H.; Feng, K.M.; Hwang, S.K. Photonic microwave carrier recovery using period-one nonlinear dynamics of semiconductor lasers for OFDM-RoF coherent detection. *Opt. Lett.* **2017**, *42*, 1482–1484.
68. Zhou, P.; Zhang, F.Z.; Guo, Q.S.; Pan, S.L. A modulator-free photonic triangular pulse generator based on semiconductor lasers. *IEEE Photon. Technol. Lett.* **2018**, *30*, 1317–1320.
69. Zhou, P.; Zhang, F.Z.; Gao, B.D.; Pan, S.L. Optical pulse generation by an optoelectronic oscillator with optically injected semiconductor laser. *IEEE Photon. Technol. Lett.* **2016**, *28*, 1827–1830.
70. Hung, Y.H.; Hwang, S.K. Photonic microwave amplification for radio-over-fiber links using period-one nonlinear dynamics of semiconductor lasers. *Opt. Lett.* **2013**, *38*, 3355–3358.
71. Hsieh, K.L.; Hwang, S.K.; Yang, C.L. Photonic microwave time delay using slow- and fast-light effects in optically injected semiconductor lasers. *Opt. Lett.* **2017**, *42*, 3307–3310.
72. Zhang, B.W.; Zhu, D.; Chen, H.; Zhou, Y.W.; Pan, S.L. Microwave Frequency Measurement Based on an Optically Injected Semiconductor Laser. *IEEE Photon. Technol. Lett.* **2020**, *32*, 1485–1488.
73. Zhou, P.; Zhang, R.H.; Li, N.Q.; Jiang, Z.D.; Pan, S.L. An RF-source-free reconfigurable microwave photonic radar with high-resolution and fast detection capability. *J. Lightwave Technol.* **2022**. [[CrossRef](#)]
74. Diaz, R.; Chan, S.C.; Liu, J.M. Lidar detection using a dual-frequency source. *Opt. Lett.* **2006**, *31*, 3600–3602. [[PubMed](#)]
75. Li, J.; Zheng, J.L.; Zhang, Y.S.; Shi, Y.C.; Zhu, H.T.; Li, Y.D.; Zhang, X.; Zhou, Y.K.; Chen, X.F. Photonic generation of linearly chirped microwave waveforms using a monolithic integrated three-section laser. *Opt. Express* **2018**, *26*, 9676–9685. [[PubMed](#)]
76. Guo, L.; Zhang, R.K.; Lu, D.; Pan, B.W.; Chen, G.G.; Zhao, L.J.; Wang, W. Linearly Chirped Microwave Generation Using a Monolithic Integrated Amplified Feedback Laser. *IEEE Photon. Technol. Lett.* **2017**, *29*, 1915–1918.
77. Huang, Y.; Zhou, P.; Li, N.Q. Broad tunable photonic microwave generation in an optically pumped spin-VCSEL with optical feedback stabilization. *Opt. Lett.* **2021**, *46*, 3147–3150.
78. Marpaung, D.; Yao, J.P.; Capmany, J. Integrated microwave photonics. *Nat. Photonics* **2019**, *13*, 80–90.